# X-ray absorption spectroscopy of single-crystalline $(VO)_2P_2O_7$: Electronic structure and possible exchange paths

S. Gerhold, N. Nücker, C. A. Kuntscher,* and S. Schuppler
*Forschungszentrum Karlsruhe, IFP, P.O. Box 3640, D-76021 Karlsruhe, Germany*

S. Stadler and Y. U. Idzerda
*Naval Research Laboratory, Code 6345, Washington DC 20375*

A. V. Prokofiev,† F. Büllesfeld, and W. Assmus
*Kristall- und Materiallabor, Physikalisches Institut, Johann Wolfgang Goethe-Universität, Robert-Mayer-Straße 2-4, D-60054 Frankfurt (Main), Germany*

(Received 16 August 2000; published 25 January 2001)

Using polarization-dependent V $2p$ and O $1s$ near-edge x-ray absorption spectroscopy, we studied the unoccupied electronic structure of single-crystalline $(VO)_2P_2O_7$. It is highly anisotropic, and shows similarities to vanadium oxides like $VO_2$ and $V_2O_5$ at the V $2p$ edge and at the O $1s$ threshold. The contributions from V-O and P-O orbitals could be identified. The results rule out the spin ladder model for the magnetic behavior of $(VO)_2P_2O_7$, but are consistent with the alternating chain scenario.

DOI: 10.1103/PhysRevB.63.073103 PACS number(s): 78.70.Dm, 71.20.Ps, 75.30.Et

Vanadyl pyrophosphate $(VO)_2P_2O_7$ (VOPO) has been receiving increased attention over the past few years, as the crystal structure[1,2] suggests that VOPO may be a realization of a spin-$\frac{1}{2}$ two-leg ladder[3] (also see Fig. 1). Indeed, first experiments on the magnetic properties of polycrystalline samples were interpreted as consistent with the ladder model.[4–6] However, quite early VOPO was also proposed to be an alternating antiferromagnetic Heisenberg spin-$\frac{1}{2}$ chain.[7] This view recently gained support from neutron-scattering experiments[8,9] that are inconsistent with the ladder model[8] and corroborate the idea of an alternating spin-$\frac{1}{2}$ chain along the *b* axis.[9,10] The chain model is also supported by electron-spin resonance and susceptibility measurements[11] obtained from large single crystals.[12] The results from Refs. 9 and 11 were further analyzed by extending the alternating chain model to include (frustrated) two-dimensional interchain coupling.[13,14] Obviously, the complex interplay between magnetic properties and the underlying structural and electronic characteristics calls for a detailed investigation of the electronic structure of VOPO—all the more as up to now just a single such study on VOPO, with a significance limited by the use of polycrystalline samples, exists in the current literature.[15] This is quite unlike the situation for vanadium oxides whose electronic structure has been analyzed in a large number of in-depth studies.

In this paper we report on near-edge x-ray absorption fine structure (NEXAFS) experiments at the V $2p$ and O $1s$ edge for VOPO. On single crystals, polarization-dependent measurements allow a detailed investigation of the unoccupied electronic structure and its anisotropy, as well as an assignment of the relevant orbitals near the Fermi energy ($E_F$). The results, in turn, are used to check if the various exchange paths implied by the different models for the magnetic behavior mentioned above are consistent with the electronic structure.

Single crystals of VOPO with a size of several $mm^3$ were grown as described in Ref. 12. For NEXAFS, the crystals were oriented by Laue diffraction to better than 1°, and (100) and (001) faces were prepared; to ensure flat and clean surfaces, several slices of about 100 nm thickness were taken off with the diamond blade of an ultramicrotome prior to the measurements. NEXAFS spectra were recorded at the National Synchrotron Light Source (NSLS) using the NRL/NSLS beamline U4B. The energy resolution was set to 210 meV at 530 eV. The bulk sensitive fluorescence yield (FY) detection mode was utilized, giving a probing depth of

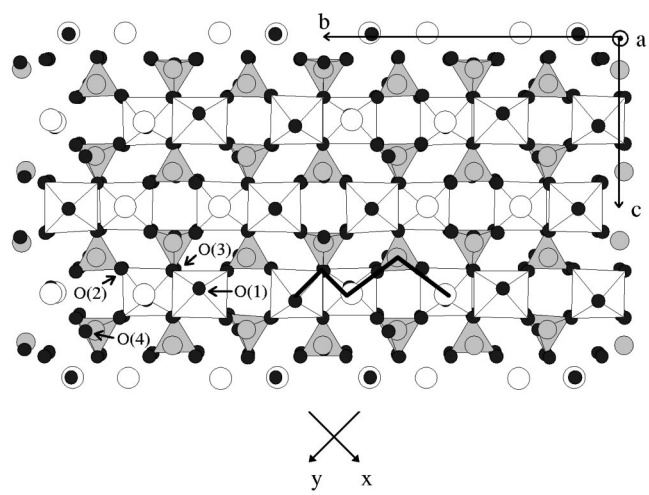


FIG. 1. Crystal structure of VOPO corresponding to Ref. 2, viewed along the *a* axis onto the (100) plane (four unit cells shown). Vanadium, phosphor, and oxygen atoms are represented by white, gray, and black circles, respectively. The (*b*,*c*) planes are stacked along the *a* axis, so that the pairs of $VO_6$ ''octahedra'' form well-separated two-leg ladders which are connected by $P_2O_7$ double tetrahedra. Note that the *x* and *y* directions are rotated by 45° with respect to the *b* and *c* crystal axes in order to align them approximately with the in-plane V-O bonds. The thick line is a sketch of a superexchange path in the alternating chain model.

 

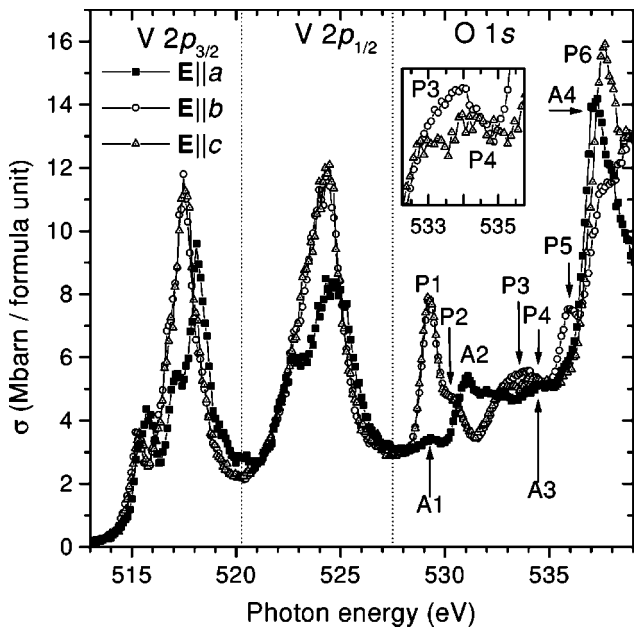


FIG. 2. V $2p$–O $1s$ FY-NEXAFS spectra for VOPO with the light polarization **E** parallel to the crystal axes *a*, *b*, and *c*. Peak labels *P* and *A* at the O $1s$ edge denote features related to the (*b*,*c*) plane and the *a* axis, respectively. The inset shows $P3$ and $P4$ for $\mathbf{E}\|(100)$ in more detail.

≈1300 Å (as calculated from tabulated atomic cross sections[16]). NEXAFS spectra were recorded simultaneously in the total electron yield mode, with the known limitations associated with that mode: (i) a small information depth of ≈40 Å (Ref. 17)—as VOPO does not cleave easily, a proper *in situ* surface preparation is not possible and adsorbates, especially at the O $1s$ edge, are likely to affect the spectra; and (ii) charging effects, since VOPO is an insulator. All experimental FY spectra shown in Fig. 2 are corrected for the incoming photon flux and for self-absorption effects, the latter by applying an extended correction scheme described elsewhere,[18] allowing one to treat a sequence of closely spaced absorption edges. Simultaneously recorded NiO spectra were referred to a NiO standard from electron-energy-loss spectroscopy,[19] resulting in an absolute energy calibration of about 0.1 eV.

The results are shown in Fig. 2 for the orientation of the polarization vector **E** parallel to the crystal axes *a*, *b*, and *c*. Further spectra with **E** oriented at angles between the axes were also recorded to test consistency, and gave the expected results: a spectrum for **E** at 45° between *b* and *c* is identical to the average of the spectra for $\mathbf{E}\|b$ and $\mathbf{E}\|c$; the $\mathbf{E}\|a$ spectra extrapolated from the $\mathbf{E}\|c$ spectrum and from spectra recorded for **E** at 45° and 60° between *c* and *a* are almost equal to the directly measured $\mathbf{E}\|a$ spectrum.

We now compare the present results with NEXAFS spectra for the vanadium oxides $VO_2$ and $V_2O_5$ (see Refs. 20 and 21), although VOPO is structurally quite different. However, the $3d^1$ configuration of the vanadium in $VO_2$ is the same, and the distortion of the $VO_6$ octahedra is very similar in $V_2O_5$, but there is no continuous network of V-O bonds in the (100) plane for VOPO. NEXAFS at the V $2p$ edge probes the local ground-state symmetry of the vanadium ion, whereas at the O $1s$ edge it gives the partial unoccupied density of states with O $2p$ character.[17,22] The shape of the V $2p$ spectra for $\mathbf{E}\|(b,c)$ is similar to that observed for $VO_2$; the intensity ratio and the angular dependence of the first two O $1s$ peaks below 532 eV is similar to $V_2O_5$. This suggests that the band-structure calculations available for $V_2O_5$ (Ref. 23) may help to assign states consisting of hybridized V $3d$–O $2p$ orbitals to characteristic features of the VOPO spectra,[24] especially as no such calculations have been published yet for VOPO.

The polarization dependent NEXAFS spectra fall in two groups with different spectral features: first the spectrum for $\mathbf{E}\|a$, i.e., with the polarization perpendicular to the layers, and second the in-plane spectra with $\mathbf{E}\|(100)$. Up to 532 eV the unoccupied electronic structure is isotropic within the (100) plane since the V $2p$ and O $1s$ spectra for $\mathbf{E}\|b$ and $\mathbf{E}\|c$ are identical in this range (see Fig. 2) and since the spectrum for **E** oriented at 45° between *b* and *c* equals the $\mathbf{E}\|b,c$ average, as mentioned above. Above 532 eV the spectra are different even within the (100) plane. Combined with the earlier argument that the first two O $1s$ features are similar to those of $V_2O_5$ spectra this observation strongly suggests that the features at the O $1s$ edge below 532 eV are related to V $3d$–O $2p$ orbitals only, and that other contributions like P $3\sigma$–O $2p$ hybrids appear above 532 eV.[25]

It is useful for a detailed discussion of the O $1s$ spectra to divide the VOPO oxygen sites into four groups (following the notation of Ref. 15; also see Fig. 1): (i) apical oxygen atoms O(1) of the distorted $VO_6$ octahedra with a short bond, $d_{\text{V-O}(1a)} \approx 1.6$ Å, and a long bond, $d_{\text{V-O}(1b)} \approx 2.3$ Å; (ii) planar oxygen atoms O(2) at the corners of the ''ladders'' with one V atom and one P atom as the nearest neighbors and $d_{\text{V-O}(2)} \approx 1.94$ Å; (iii) planar oxygen atoms O(3) forming the ''ladder rungs'' with two V and one P atom as nearest neighbors, and $d_{\text{V-O}(3)} \approx 2.07$ Å; and (iv) O(4) concatenating two $PO_4$ tetrahedra to form the $P_2O_7$ group.

For vanadium oxides like $VO_2$ and $V_2O_5$ the first and second peaks at the O $1s$ edge are ascribed to O $2p$ orbitals hybridized with the $t_{2g}$ and $e_g$ subgroups of the unoccupied V $3d$ orbitals, respectively; they are separated by an octahedral ligand field splitting of about 2.2 eV.[21] This picture can directly be transferred to the case of VOPO in Fig. 2 [labeling spectral features for **E** parallel to the (100) plane by *P* and those for $\mathbf{E}\|a$ by *A*]: peaks $P1$ and $A1$ correspond to $t_{2g}$ states, whereas the features $P2$ and $A2$ correspond to $e_g$ states. $P1$ is located at 529.1 eV, $P2$ is just a shoulder at 530.5 eV, and $A1$ and $A2$ are located at 529.2 and 531 eV, respectively. A peak shift for different orientations like the one between $P2$ and $A2$ is not observed for $V_2O_5$.[20,21] The ligand field splitting for VOPO determined from the separation of the first and second O $1s$ peaks is about $1.6 \pm 0.2$ eV and thus smaller than for the vanadium oxides mentioned above. In order to interpret peaks $A1$ to $P2$ we can use Ref. 23 as a guide (also see Table I). Note that the notation used for the orbitals is in the local *x*, *y*, and *z* basis set depicted in Fig. 1, where the in-plane *x* and *y* axes are rotated by 45° against the in-plane *b* and *c* axes; *a* is parallel to *z*. The main

contribution to $P1$ is due to V $3d_{xy}$–O(2,3) $2p_{x,y}\pi$ orbitals; from symmetry considerations and in analogy to Ref. 23 V $3d_{xz,yz}$–O($1a$) $2p_{x,y}\pi$ contributions are also likely to occur. $P2$ is assigned to V $3d_{x^2\text{-}y^2}$–O(2,3) $2p_{x,y}\sigma$ orbitals. $A1$ is due to V $3d_{xz,yz}$–O(2,3) $2p_z\pi$ orbitals, and $A2$ can safely be attributed to V $3d_{3z^2\text{-}r^2}$–O($1a$) $2p_z\sigma$ orbitals. A contribution of V $3d_{3z^2\text{-}r^2}$–O($1b$) $2p_z\sigma$ orbitals is unlikely, as $A2$ lies about 0.5 eV *higher* in energy than $P2$, which is, in an approximate $D_{4h}$ environment, possible only for a dominant V-O(1a) hybridization;[26] this is consistent with the strong $d$ dependence of the $pd\sigma$ hybridization.[27] The symmetric occurrence of $x$ and $y$ labels in all pertinent orbitals reflects the isotropy of the in-plane spectra.

We will now concentrate on the spectral weight above 532 eV. The V $4sp$–O $2p$ antibonding bands give a nearly isotropic contribution to the absorption structures, and are responsible for most of the spectral weight of the main peak above 535 eV.[15,21] The spectral weight between 532 and 535 eV and the anisotropic part above 535 eV should be assigned to P $3\sigma$–O $2p$ antibonding orbitals (cf. Table II). O(1) will not contribute, as it does not bond to phosphor atoms. When trying to unravel possible P-O(2) contributions to polarization-dependent NEXAFS along the crystal axes we note that the lines connecting neighboring P and O(2) enclose angles of about 33°–45° with the $b$ axis, and lie almost perpendicular to $a$. The most likely hybridization is P $3\sigma$–O(2) $2p_x$ [or $P$ $3\sigma$–O(2) $2p_y$, depending on which specific O(2) site out of the 16 inequivalent ones is being considered]; accounting for the slightly different angles these orbitals will contribute 50–70 % to the $\mathbf{E}\|b$ spectra and 30–50 % to $\mathbf{E}\|c$. We indeed observe two features fulfilling this condition: a well-developed peak $P3$ at 533.7 eV for $\mathbf{E}\|b$, where for $\mathbf{E}\|c$ only a strong shoulder on the low energy side of $P4$ is present and the prominent feature $P5$ at 535.9 eV close below the main peak for $\mathbf{E}\|b$. Similarly, the line connecting neighboring P and O(3) is oriented almost completely along $c$. The hybridization can take place with a symmetric combination of O $2p_x$ and O $2p_y$ orbitals and should show up in NEXAFS mostly in the $\mathbf{E}\|c$ spectrum. Indeed, such a spectral weight appears as a small peak $P4$ around 534.2 eV for $\mathbf{E}\|c$, where the quite broad feature $P3$ for $\mathbf{E}\|b$ is simply falling off without any extra structures, and more prominently around 537.5 eV ($P6$). In the same manner, for O(4) only P $3\sigma$–O(4) $2p_z$ contributions to the $\mathbf{E}\|a$ spectrum are possible: they can be observed as a weak peak $A3$ at 534.4 eV, and more pronounced at 537.2 eV ($A4$). The fact that each kind of P-O bonds just discussed seems to give rise to spectral weight at *two* different energies might reflect the ligand field splitting of the V $3d$ orbitals, mediated by the V-O-P hybridization: the same O $2p$ orbitals are involved both in the V-derived $t_{2g}$ and $e_g$ peaks as well as in the P $3\sigma$–O $2p$ peaks. This would support the suggestion of coherent molecular orbitals providing the superexchange path via the $PO_4$ groups in VOPO.[28] Alternatively, the energetically higher peak of each pair could also be due to P $3d$–O $2p$ hybrids.

With these assignments of the unoccupied electronic structure near threshold one can now test if and to what extent they are compatible with the magnetic interactions implied by the various models for the magnetic behavior of VOPO. For a reasonable exchange coupling of two adjacent vanadium spins there must be sufficient ''hybridization strength'' as well as unoccupied density of states for all bonds involved along the exchange path.[29] The ladder model requires V-O(1)-V paths along the legs of the ladder and V-O(3)-V paths along the rungs. As there are no signs for a significant V-O(1b) hybridization the V-O(1)-V path must be very weak, and thus the spin ladder model can clearly be excluded by our NEXAFS results. This agrees with the latest experiments on magnetic properties.[8,9,11,13,14] On the other hand, the model of an alternating chain along $b$ (see Refs. 9 and 14) requires V-O(2)-P-O(2)-V and V-O(3)-V paths (depicted as a heavy solid line in Fig. 1). If, as suggested in Ref. 14, the chains are additionally coupled along $a$ there has to be a V-O(2)-P-O(4)-P-O(2)-V path as well; its analogs, involving O(3) instead of O(2), can be excluded by noting that they would, at the same time, lead to an additional V-O(3)-P-O(2)-V coupling along $c$ which is experimentally not observed.[14] Our NEXAFS data are consistent with these models, first because all relevant V-O and P-O hybridizations are shown to be present, and second because the R-O(3) hybrids exhibit less pronounced features than the P-O(2) hybrids as discussed above. A further distinction in NEXAFS between the individual contributions from the two classes of crystallographically slightly inequivalent chains[30,31] is not possible: although each single absorption process is local the information is averaged over all these crystallographically inequivalent sites (due to the macroscopic beam spot size and the large penetration depth).

In summary, polarization-dependent NEXAFS at the V $2p$ and O $1s$ edges for single-crystalline VOPO shows that the unoccupied electronic structure is highly anisotropic. The

TABLE I. Assignment of the observed O $1s$ near-edge peaks to V $3d$–O $2p$ hybridized orbitals.

| | | Vanadium | | | | |
|---|---|---|---|---|---|---|
| | | | $t_{2g}$ | | $e_g$ | |
| | | $3d_{xy}$ | $3d_{xz}$ | $3d_{yz}$ | $3d_{x^2-y^2}$ | $3d_{3z^2-r^2}$ |
| O(1) | $2p_x$ | | $P1$ | | | |
| | $2p_y$ | | | $P1$ | | |
| | $2p_z$ | | | | | $A2$ |
| O(2,3) | $2p_x$ | $P1$ | | | $P2$ | |
| | $2p_y$ | $P1$ | | | $P2$ | |
| | $2p_z$ | | $A1$ | $A1$ | | |

TABLE II. Assignment of the observed peaks at the O $1s$ edge above 532 eV to P $3\sigma$–O $2p$ hybridized orbitals.

| | | P $3\sigma$ |
|---|---|---|
| O(2) | $2p_{x,y}$ | $P3/P5$ |
| O(3) | $2p_{(x+y)/\sqrt{2}}$ | $P4/P6$ |
| O(4) | $2p_z$ | $A3/A4$ |

orbital character of the features observed close to the O $1s$ edge is V $3d$ derived; states with P $3\sigma$ character start to appear at somewhat higher energy. The energetic sequence observed for the crystal-field split $e_g$ levels shows that the V-O(1b) hybridization is negligible, and thus that VOPO is not a spin ladder. Our results are consistent with the now generally accepted models describing VOPO as an alternating spin chain.

Fruitful discussions with E. Pellegrin, as well as his critical reading of this manuscript, are gratefully acknowledged. We thank J.-H. Park and S. L. Hulbert for valuable experimental help. Research was carried out in part at the National Synchrotron Light Source, Brookhaven National Laboratory, which is supported by the U.S. Department of Energy, Division of Material Sciences and Division of Chemical Sciences, under Contract No. DE-AC02-98CH10886.

*Present address: 1. Physikalisches Institut, Universität Stuttgart, Pfaffenwaldring 57, D-70550 Stuttgart, Germany.

†Guest scientist from A. F. Ioffe Physical Technical Institute, St. Petersburg 194021, Russia.

[1] Y. E. Gorbunova and S. A. Linde, Dokl. Akad. Navk. Nauk. SSSR **245**, 584 (1978) [Sov. Phys. Dokl. **24**, 138 (1979)].

[2] P. T. Nguyen, R. D. Hofmann, and A. W. Sleight, Mater. Res. Bull. **30**, 1055 (1995).

[3] E. Dagotto and T. M. Rice, Science **271**, 618 (1996).

[4] R. S. Eccleston, T. Barnes, J. Brody, and J. W. Johnson, Phys. Rev. Lett. **73**, 2626 (1994).

[5] J. Kikuchi, T. Yamauchi, and Y. Ueda, J. Phys. Soc. Jpn. **66**, 1622 (1997).

[6] R. C. Eccleston and M. J. Steiner, Physica B **234-236**, 544 (1997).

[7] D. C. Johnston, J. W. Johnson, D. P. Goshorn, and A. J. Jacobson, Phys. Rev. B **35**, 219 (1987).

[8] A. W. Garrett, S. E. Nagler, T. Barnes, and B. C. Sales, Phys. Rev. B **55**, 3631 (1997).

[9] A. W. Garrett, S. E. Nagler, D. A. Tennant, B. C. Sales, and T. Barnes, Phys. Rev. Lett. **79**, 745 (1997).

[10] The experiments in Ref. 9 were performed with a matrix of oriented small single crystals.

[11] A. V. Prokofiev, F. Büllesfeld, W. Assmus, H. Schwenk, D. Wichert, U. Löw, and B. Lüthi, Eur. Phys. J. B **5**, 313 (1998).

[12] A. V. Prokofiev, F. Büllesfeld, and W. Assmus, Cryst. Res. Technol. **33**, 157 (1998).

[13] A. Weisse, G. Bouzerar, and H. Fehske, Eur. Phys. J. B **7**, 5 (1999).

[14] G. S. Uhrig and B. Normand, Phys. Rev. B **58**, R14 705 (1998).

[15] X. W. Lin, Y. Y. Wang, V. P. Dravid, P. M. Michalakos, and M. C. Kung, Phys. Rev. B **47**, 3477 (1993).

[16] W. J. Veigele, in *Handbook of Spectroscopy*, edited by J. W. Robinson (CRC Press, Cleveland, 1974), Vol. 1, p. 28.

[17] F. M. F. de Groot, J. Electron Spectrosc. Relat. Phenom. **67**, 529 (1994).

[18] S. Gerhold, C. A. Kuntscher, G. Linker, M. Merz, N. Nücker, C. A. Kuntscher, S. Schuppler, S. Stadler, Y. U. Idzerda, W. H. Tang, J. Gao, A. Attenberger, H. Berger, A. V. Prokofiev, F. Büllesfeld, and W. Assmus (unpublished).

[19] M. Knupfer (private communication).

[20] E. Goering, O. Müller, M. L. den Boer, and S. Horn, Physica B **194–196**, 1217 (1994).

[21] R. Zimmermann, R. Claessen, F. Reinert, P. Steiner, and S. Hüfner, J. Phys.: Condens. Matter **10**, 5697 (1998).

[22] F. M. F. de Groot, J. Electron Spectrosc. Relat. Phenom. **62**, 111 (1993).

[23] V. Eyert and K.-H. Höck, Phys. Rev. B **57**, 12727 (1998).

[24] The applicability of parts of the $V_2O_5$ band structure calculation to VOPO is also limited by the different $3d$ occupancies of the vanadium ion.

[25] Following the notation of Ref. 15, we denote the P $3sp^3$ orbitals by P $3\sigma$.

[26] For a contracted $VO_6$ octahedron the $3d_{3z^2\text{-}r^2}$ orbital lies higher in energy than the $3d_{x^2\text{-}y^2}$ orbital; for an elongated octahedron the situation is reversed. For equally strong V-O (1a) and V-O (1b) bonds one would expect broadened $e_g$ peaks at the same energy position for $\mathbf{E}\|a$ and for $\mathbf{E}\|(100)$, in contrast to the experimental observations.

[27] W. A. Harrison, *Electronic Structure and the Properties of Solids* (Freeman, San Francisco, 1980).

[28] D. Beltrán-Porter, P. Amorós, R. Ibáñez, E. Martínez, and A. Beltrán-Porter, Solid State Ionics **32/33**, 57 (1989).

[29] P. W. Anderson, Phys. Rev. **79**, 350 (1950).

[30] Z. Hiroi, M. Azuma, Y. Fujishiro, T. Saito, M. Takano, F. Izumi, T. Kamiyama, and T. Ikeda, J. Solid State Chem. **146**, 369 (1999).

[31] J. Kikuchi, K. Motoya, T. Yamauchi, and Y. Ueda, Phys. Rev. B **60**, 6731 (1999).